

Projection-Based Memory Kernel Coupling Theory for Quantum Dynamics: A Stable Framework for Non-Markovian Simulations

Wei Liu,¹ Rui-Hao Bi,¹ Yu Su,² Limin Xu,³ Zhennan Zhou,³ Yao Wang,² and Wenjie Dou^{1, 4, 5, a)}

¹⁾Department of Chemistry, School of Science and Research Center for Industries of the Future, Westlake University, Hangzhou, Zhejiang 310030, China

²⁾Hefei National Research Center for Physical Sciences at the Microscale, University of Science and Technology of China, Hefei, Anhui 230026, China

³⁾Institute for Theoretical Sciences, Westlake University, Hangzhou, 310030, China

⁴⁾Institute of Natural Sciences, Westlake Institute for Advanced Study, Hangzhou, Zhejiang 310024, China

⁵⁾Key Laboratory for Quantum Materials of Zhejiang Province, Department of Physics, School of Science and Research Center for Industries of the Future, Westlake University, Hangzhou, Zhejiang 310030, China

(Dated: 12 February 2026)

We present a projection-based, stability-preserving methodology for computing time correlation functions in open quantum systems governed by generalized quantum master equations with non-Markovian effects. Building upon the memory kernel coupling theory framework, our approach transforms the memory kernel hierarchy into a system of coupled linear differential equations through Mori-Zwanzig projection, followed by spectral projection onto stable eigenmodes to ensure numerical stability. By systematically eliminating unstable modes while preserving the physically relevant dynamics, our method guarantees long-time convergence without introducing artificial damping or *ad hoc* modifications. The theoretical framework maintains mathematical rigor through orthogonal projection operators and spectral decomposition. Benchmark calculations on the spin-boson model show excellent agreement with exact hierarchical equations of motion results while achieving significant computational efficiency. This approach provides a versatile and reliable framework for simulating non-Markovian dynamics in complex systems.

I. INTRODUCTION

The simulation of open quantum systems—quantum subsystems interacting with complex, macroscopic environments—represents a significant challenge in modern theoretical chemistry, condensed matter physics, and quantum information science^{1,2}. Such systems govern a diverse variety of phenomena, from ultrafast excitonic energy transfer in photosynthetic complexes³ to quantum transport and decoherence in nanoscale electronic devices^{4,5}, where non-Markovian memory effects and system-environment correlations often play essential roles^{6–9}. At the heart of these processes lies the time correlation function, a fundamental quantity that directly links microscopic quantum dynamics to experimentally accessible spectroscopic observables, transport coefficients, and thermalization rates^{10–18}.

Despite significant methodological advances, there is a long-standing dilemma between accuracy and computational tractability in quantum dynamics simulations. On the one hand, numerically exact approaches, such as the hierarchical equations of motion (HEOM)², the dissipation equation of motion (DEOM)¹⁹ and real-time path integral techniques^{20,21}, suffer from high computational scaling with system size or memory time, limiting their application to relatively small systems. On the other hand, widely used approximate methods—including per-

turbative master equations^{22–24} and mixed quantum-classical schemes^{25–29}—often achieve favorable scaling by sacrificing accuracy, especially in non-perturbative regimes, or by violating fundamental physical principles such as detailed balance and positivity.

Projection operator techniques^{30–32} offer an elegant theoretical framework to tackle this difficulty. By formally partitioning the full dynamics into relevant and irrelevant parts, these methods recast the exact dynamics into a generalized quantum master equation (GQME) for the reduced density matrix³³. The memory kernel $K(t)$ within the GQME encodes all non-Markovian effects and typically decays faster than the reduced system's observables, providing a potential avenue for computational leverage^{5,34}. However, practical computation of $K(t)$ remains formidable, as it requires propagating dynamics in the formally exact orthogonal subspace.

Recent advances in memory kernel coupling theory (MKCT)^{35,36} have introduced a promising reformulation. MKCT expresses the memory kernel dynamics through a hierarchy of coupled equations of motion, driven by *static* moments. Such a transformation from a dynamical evolution into a static one offers significant conceptual and potential computational advantages. Nevertheless, practical implementations of MKCT are plagued by severe numerical instabilities upon truncation of the hierarchy^{37–39}. Current stabilization strategies rely on empirically tuned methods, such as Padé approximants³⁶ or dynamical mode decomposition (DMD)^{35,40}, which do not always guarantee convergence.

In this work, we introduce the projection-based mem-

^{a)}Electronic mail: douwenjie@westlake.edu.cn

ory kernel coupling theory (PMKCT)—a mathematically rigorous stabilization framework that guarantees numerical stability while intrinsically preserving necessary physical constraints for the memory kernel. The core innovation of PMKCT lies in a spectral decomposition of the MKCT generator matrix, segregating its dynamics into stable and unstable subspaces. A subsequent projection step systematically removes the unstable modes responsible for numerical divergence, transforming an *ad hoc* numerical problem into a principled linear algebraic operation with only the stable modes. Our approach completely eliminates empirical parameter tuning and fully retains the computational advantages and formal structure of the original MKCT formalism.

The remainder of this paper is organized as follows. In Section II, we develop the complete PMKCT framework, detailing the spectral analysis of the MKCT generator and the projection-based stabilization procedure. Section III presents comprehensive numerical benchmarks on the widely studied spin-boson model, comparing PMKCT against established exact methods. Finally, we conclude in Section IV by summarizing our key contributions and discussing the broader implications of PMKCT for the future simulation of complex open quantum systems.

II. THEORETICAL FRAMEWORK

A. Generalized Quantum Master Equation

Our framework builds upon the Mori-Zwanzig projection formalism³², which provides an exact representation of open quantum system dynamics. For an observable \hat{A} , the GQME reads:

$$\dot{C}_{\hat{A}\hat{A}}(t) = \Omega C_{\hat{A}\hat{A}}(t) + \int_0^t d\tau K(t-\tau) C_{\hat{A}\hat{A}}(\tau), \quad (1)$$

where $C_{\hat{A}\hat{A}}(t) = \langle \hat{A}(t)\hat{A}(0) \rangle$ is the correlation function, $\Omega = \langle i\mathcal{L}\hat{A}\hat{A} \rangle / \langle \hat{A}\hat{A} \rangle$ is the frequency parameter, and $K(t) = \langle i\mathcal{L}e^{it\mathcal{Q}\mathcal{L}}Q i\mathcal{L}\hat{A}\hat{A} \rangle / \langle \hat{A}\hat{A} \rangle$ is the memory kernel. The Liouville operator \mathcal{L} acts as $\mathcal{L}\hat{X} = [\hat{H}, \hat{X}]/i\hbar$, and $\mathcal{Q} = I - \mathcal{P}$ is the complement of the projection operator $\mathcal{P}\hat{X} = \langle \hat{X}\hat{A} \rangle \hat{A} / \langle \hat{A}\hat{A} \rangle$. The inner product is given by $\langle \hat{O}_1 \hat{O}_2 \rangle \equiv \text{Tr}(\hat{O}_1 \hat{O}_2 \rho_{ss})$, where ρ_{ss} is the steady state.

The memory kernel $K(t)$ encodes the non-Markovian influence of the environment and typically decays faster than $C_{\hat{A}\hat{A}}(t)$ itself, offering computational advantages. However, computing $K(t)$ remains challenging as it involves the projected propagator $e^{it\mathcal{Q}\mathcal{L}}$ in the orthogonal subspace.

B. Memory Kernel Coupling Theory

MKCT³⁵ provides a systematic approach for computing $K(t)$ by introducing auxiliary kernels. Defining the

nth-order moment:

$$\Omega_n \equiv \langle (i\mathcal{L})^n \hat{A}\hat{A} \rangle / \langle \hat{A}\hat{A} \rangle, \quad (2)$$

and the n th-order auxiliary kernel:

$$K_n(t) \equiv \langle (i\mathcal{L})^n \hat{f}(t) \hat{A} \rangle / \langle \hat{A}\hat{A} \rangle, \quad \hat{f}(t) = e^{it\mathcal{Q}\mathcal{L}}Q i\mathcal{L}A, \quad (3)$$

the following hierarchy emerges³⁵:

$$\dot{K}_n(t) = K_{n+1}(t) - \Omega_n K_1(t), \quad n = 1, \dots, N, \quad (4a)$$

$$K_n(0) = \Omega_{n+1} - \Omega_n \Omega_1. \quad (4b)$$

The above equations form a semi-infinite chain that resembles HEOM. In practice, proper truncation has to be introduced. In the following, we set $K_{N+1}(t) = 0$. Note that this formulation elegantly separates static moment computation (Ω_n) from time evolution, with the latter governed by a linear system. In matrix form with $\mathbf{K}(t) = [K_1(t), \dots, K_N(t)]^\top$:

$$\dot{\mathbf{K}}(t) = M\mathbf{K}(t), \quad (5)$$

with the initial condition $\mathbf{K}(0) = [\Omega_2 - \Omega_1^2, \Omega_3 - \Omega_2\Omega_1, \dots, \Omega_{N+1} - \Omega_N\Omega_1]^\top$, and M has the specific structure

$$M_{ij} = \delta_{i+1,j} - \Omega_i \delta_{j,1}, \quad (6)$$

explicitly:

$$M = \begin{pmatrix} -\Omega_1 & 1 & 0 & \cdots & 0 \\ -\Omega_2 & 0 & 1 & \cdots & 0 \\ \vdots & \vdots & \ddots & \ddots & \vdots \\ -\Omega_{N-1} & 0 & \cdots & 0 & 1 \\ -\Omega_N & 0 & \cdots & 0 & 0 \end{pmatrix}_{N \times N}. \quad (7)$$

The formal solution is $\mathbf{K}(t) = \exp(Mt)\mathbf{K}(0)$, with $K_1(t)$ corresponding to the physical memory kernel in Eq. (1).

C. Stability Challenge and Projection-Based Solution

While Eq. (5) provides an exact representation for infinite N , truncation to finite N introduces eigenvalues with positive real parts, causing exponential divergence. This numerical instability represents a fundamental limitation of practical MKCT implementations. In previous study, we have used DMD³⁵ or Padé³⁶ to remove the divergence. In the following, we introduce the projection based method.

Our projection-based approach addresses this by systematically decomposing the dynamics into stable and unstable components. Consider the spectral decomposition $M = V\Lambda V^{-1}$ with eigenvalues λ_i . We classify:

$$\mathcal{S} = \{\lambda_i : \Re(\lambda_i) < 0\} \quad (\text{stable}), \quad (8)$$

$$\mathcal{N} = \{\lambda_i : \Re(\lambda_i) = 0\} \quad (\text{neutral}), \quad (9)$$

$$\mathcal{U} = \{\lambda_i : \Re(\lambda_i) > 0\} \quad (\text{unstable}). \quad (10)$$

Let V_S contain eigenvectors for $\mathcal{S} \cup \mathcal{N}$. The orthogonal projection onto $\mathcal{V}_S = \text{span}(V_S)$ is^{41,42}:

$$P_S = V_S (V_S^\dagger V_S)^{-1} V_S^\dagger. \quad (11)$$

Applying this projection yields the stabilized system:

$$\dot{\mathbf{K}}(t) = M_S \mathbf{K}(t), \quad (12a)$$

$$M_S = P_S M P_S, \quad (12b)$$

with solution $\mathbf{K}(t) = \exp(M_S t) \mathbf{K}(0)$.

For the projected system, $\sigma(M_S) \subseteq \{\lambda \in \mathbb{C} : \Re(\lambda) \leq 0\}$, and any eigenvalues with $\Re(\lambda) = 0$ are semisimple. M_S acts invariantly on \mathcal{V}_S with spectrum $\sigma(M_S) = \sigma(M) \cap (\mathcal{S} \cup \mathcal{N})$. The orthogonal projection ensures neutral eigenvalues are non-defective.

The reason why one can project out the unstable modes is tied to the breakdown of time-reversal symmetry. For open quantum systems, the time reversibility is violated. However, such time reversibility is preserved in the original MKCT. By removing the unstable modes, one introduces breakdown of time-reversal symmetry in MKCT. Notice that introducing breakdown of time-reversal symmetry is also essential in DEOM. In DEOM, the Wick theorem is used differently for positive time and negative time.¹⁹ Below, we show that this projected based method works in practice.

D. Numerical Implementation Considerations

For improved numerical conditioning with large N , particularly when Ω_n span multiple orders of magnitude, we employ variable rescaling^{43–45}. Two effective schemes are presented below, each with its distinct matrix representation.

1. Factorial Scaling Scheme

Define scaled variables $\tilde{K}_n(t) = K_n(t)/(n! \Lambda^{n-1})$ with characteristic frequency Λ . The transformed hierarchy becomes:

$$\dot{\tilde{K}}_n(t) = (n+1) \Lambda \tilde{K}_{n+1}(t) - \frac{\Omega_n}{n! \Lambda^{n-1}} \tilde{K}_1(t), \quad (13)$$

with $\tilde{K}_{N+1}(t) = 0$. In matrix form with $\tilde{\mathbf{K}}(t) = [\tilde{K}_1(t), \dots, \tilde{K}_N(t)]^\top$:

$$\frac{d}{dt} \tilde{\mathbf{K}}(t) = \tilde{M}^{(1)} \tilde{\mathbf{K}}(t), \quad (14)$$

where the $N \times N$ matrix $\tilde{M}^{(1)}$ has elements:

$$\tilde{M}_{ij}^{(1)} = (i+1) \Lambda \delta_{i+1,j} - \frac{\Omega_i}{i! \Lambda^{i-1}} \delta_{j,1}. \quad (15)$$

2. Power-Law Scaling Scheme

For $\tilde{K}_n(t) = K_n(t)/\Lambda^{n-1}$, we obtain:

$$\dot{\tilde{K}}_n(t) = \Lambda \tilde{K}_{n+1}(t) - \frac{\Omega_n}{\Lambda^{n-1}} \tilde{K}_1(t), \quad (16)$$

with $\tilde{K}_{N+1}(t) = 0$. The corresponding matrix $\tilde{M}^{(2)}$ has elements:

$$\tilde{M}_{ij}^{(2)} = \Lambda \delta_{i+1,j} - \frac{\Omega_i}{\Lambda^{i-1}} \delta_{j,1}. \quad (17)$$

3. Projection Framework Compatibility

The projection stabilization procedure established in Section II C applies directly to both rescaled formulations. For $\tilde{M}^{(k)} \in \{\tilde{M}^{(1)}, \tilde{M}^{(2)}\}$, we compute stabilized matrices via:

$$\tilde{M}_S^{(k)} = P_S^{(k)} \tilde{M}^{(k)} P_S^{(k)}, \quad (18)$$

where $P_S^{(k)}$ denotes the projection operator constructed from stable eigenvectors of $\tilde{M}^{(k)}$. This maintains mathematical consistency across all formulations while improving numerical conditioning.

4. Physical Kernel Extraction

A key advantage of both rescaling schemes is the trivial recovery of the physical memory kernel:

$$K_1(t) = \tilde{K}_1(t), \quad (19)$$

since scaling factors cancel precisely for $n = 1$. No inverse transformation is required, providing direct access to the physically meaningful quantity. Higher-order auxiliary kernels ($n > 1$) serve exclusively as numerical intermediaries to ensure stability; they possess no independent physical significance and need not be recovered explicitly.

III. RESULTS AND DISCUSSION

We validate our PMKCT framework on the spin-boson model with Ohmic spectral density, described by the Hamiltonian $H = H_S + H_{SB} + h_B = H_S + \hat{Q}\hat{F} + h_B$, where H_S and h_B are the system Hamiltonian and the bath Hamiltonian, and H_{SB} is the coupling between the system and bath. \hat{Q} is a system operator σ_x and \hat{F} is an environment operator, which are both Hermitian. We have

$$\begin{aligned} H_S &= \frac{1}{2} \Delta \sigma_z + \epsilon \sigma_x, \\ h_B &= \sum_j \frac{1}{2} \omega_j (\hat{p}_j^2 + \hat{x}_j^2), \\ \hat{F} &= \sum_j c_j \hat{x}_j. \end{aligned} \quad (20)$$

Here, Δ is the unit energy, which corresponds to the energy difference between the two sites. ϵ represents the tunneling matrix element, which is assumed to be static. And σ_i corresponds to the i^{th} Pauli matrix. p_j , x_j , and ω_j are the momenta, coordinates, and frequency for the j^{th} harmonic oscillator, respectively. c_j is the coupling constant that describes the strength of the interaction between the system and the j^{th} oscillator. The initial state $\hat{\sigma}_0 = |0\rangle\langle 0|$. We compute the dipole autocorrelation function $C_{\hat{\mu}\hat{\mu}}(t) = \langle \hat{\sigma}_x(t)\hat{\sigma}_x(0) \rangle$, where the absorption lineshape is obtained via Fourier transform:

$$I(\omega) \propto \Re \int_0^\infty dt C_{\hat{\mu}\hat{\mu}}(t) e^{i\omega t}. \quad (21)$$

The system-bath interaction is fully characterized by the Ohmic spectral density,

$$J(\omega) = 2\gamma\omega e^{-|\omega|/\omega_D}, \quad (22)$$

where γ controls coupling strength and ω_D is the cutoff frequency. Throughout, we set $\hbar = 1$.

A. Stability Analysis and Eigenvalue Spectra

In Fig. 1, we demonstrate the stabilization effect of PMKCT for the spin-boson model. The original matrix M with $N = 40$ exhibits 21 eigenvalues with positive real parts (Fig. 1a), which would cause exponential divergence in direct integration. After applying our projection procedure, all eigenvalues of M_S reside in the left half-plane (Fig. 1b), guaranteeing asymptotic stability.

The number of unstable modes increases with truncation order N , as shown in Table I. This highlights the importance of stabilization for accurate long-time simulations.

TABLE I: Unstable modes in original M versus truncation order N

N	10	20	30	40
Unstable modes	5	10	15	21
$\max_{\lambda \in \mathcal{U}} \Re(\lambda)$	0.199	0.202	0.206	0.217
$\min_{\lambda \in \mathcal{U}} \Re(\lambda)$	0.057	0.031	0.026	0.006

B. Memory Kernel and Correlation Function Dynamics

In Fig. 2, we compare PMKCT results with numerically exact dissipaton equation of motion (DEOM)¹⁹ calculations. For the memory kernel $K_1(t)$ (Fig. 2a and Fig. 2b), PMKCT achieves excellent agreement with DEOM across the entire time range.

The correlation function $C_{\hat{\mu}\hat{\mu}}(t)$ (Fig. 2c and Fig. 2d) exhibits rapid oscillations due to the large energy gap ($\Delta = 20$). PMKCT captures these oscillations accurately.

A key observation is that $K_1(t)$ decays significantly faster than $C_{\hat{\mu}\hat{\mu}}(t)$, decaying to near-zero by $t \approx 2$, while $C_{\hat{\mu}\hat{\mu}}(t)$ maintains substantial amplitude beyond $t = 10$. This rapid kernel decay is exploited in both PMKCT and MKCT frameworks for efficient long-time simulations.

C. Convergence with Truncation Order

In Fig. 3, we investigate the convergence of the PMKCT method as the truncation order N increases. The error of memory kernel decreases with larger N , which aligns with the theoretical expectations for continued fraction truncation. For this parameter set, an absolute error within 10^{-7} is achieved at $N = 40$.

D. Frequency-Domain Analysis

In Fig. 4, we present frequency-domain results. The memory kernel spectrum $K_1(\omega)$ (Figs. 4a, 4b and 4c) displays a broad distribution centered around $\omega \approx \Delta = 20$, with significant weight extending to higher frequencies. This broad spectrum reflects the non-Markovian character of the dynamics. Due to the projection operation, the memory kernel of PMKCT exhibits oscillations in the frequency range of 10–40 (on the x-axis). However, these oscillations do not affect the peak positions in the resulting absorption lineshape.

The absorption lineshape $I(\omega)$ (Fig. 4d) shows the expected peak structure, with PMKCT accurately reproducing the DEOM reference. The slight asymmetry arises from the finite temperature ($\beta = 5$) and Ohmic bath characteristics.

IV. CONCLUSIONS

We have developed a projection-based memory kernel coupling theory (PMKCT) that provides a stable, efficient framework for simulating non-Markovian quantum dynamics. Building upon the MKCT formalism, our approach employs spectral projection techniques to guarantee numerical stability by construction while maintaining physical consistency. The principal contributions are: establishing a rigorous mathematical framework based on orthogonal projection operators and spectral theory and ensuring guaranteed asymptotic stability through systematic elimination of unstable modes.

PMKCT enables accurate long-time simulations of complex open quantum systems, as demonstrated on the spin-boson model with linear couplings. The method provides a systematic alternative to empirical truncation schemes like Padé approximants, offering guaranteed convergence without parameter tuning. Future extensions will target larger systems and more complex interactions, with applications spanning quantum materials, chemical dynamics, and biological systems.

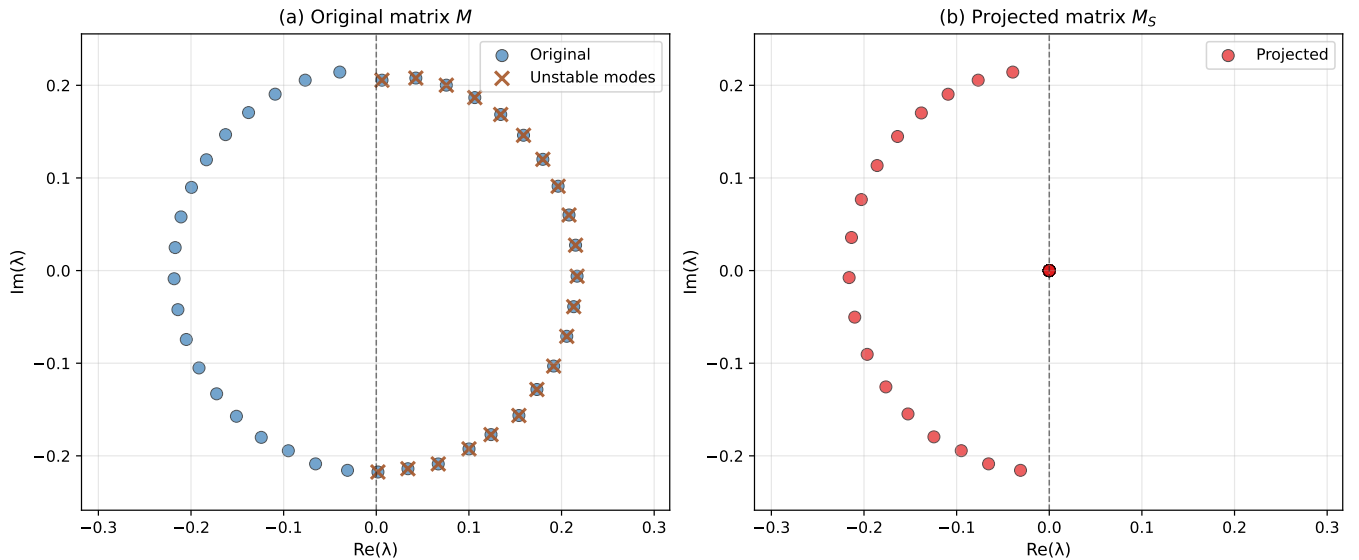


FIG. 1: Eigenvalue spectra for the spin-boson model with $\Delta = 20$, $\gamma = 0.5$, $\omega_D = 1$, $\beta = 5$, $N = 40$. Power-law scaling is used with $\Lambda = 100$. (a) Original matrix M shows 21 eigenvalues with $\Re(\lambda) > 0$ (crosses). (b) After projection, all eigenvalues satisfy $\Re(\lambda) \leq 0$.

ACKNOWLEDGMENTS

We thank Jian-Guo Liu and Xu'an Dou for useful discussions. This work was supported by the National Natural Science Foundation of China (Grant Nos. 22361142829, 22273075) and the Zhejiang Provincial Natural Science Foundation (Grant No. XHD24B0301). Computational resources were provided by the Westlake University Supercomputer Center.

AUTHOR DECLARATIONS

Conflict of Interest

The authors have no conflicts to disclose.

- ¹Y. Wang and Y. Yan, “Quantum mechanics of open systems: Dissipation theories,” *The Journal of Chemical Physics* **157** (2022).
- ²Y. Tanimura, “Numerically “exact” approach to open quantum dynamics: The hierarchical equations of motion (heom),” *The Journal of chemical physics* **153** (2020).
- ³T. Renger, V. May, and O. Kühn, “Ultrafast excitation energy transfer dynamics in photosynthetic pigment–protein complexes,” *Physics Reports* **343**, 137–254 (2001).
- ⁴J. Chen, W. Liu, V. Mosallanejad, and W. Dou, “Floquet non-adiabatic nuclear dynamics with photoinduced lorentz-like force in quantum transport,” *The Journal of Physical Chemistry C* **128**, 11219–11228 (2024).
- ⁵W. Liu, J. Chen, and W. Dou, “Enhancement of chiral-induced spin selectivity via circularly polarized light,” *The Journal of Physical Chemistry C* **129**, 10181–10188 (2025).
- ⁶X. Li, S.-X. Lyu, Y. Wang, R.-X. Xu, X. Zheng, and Y. Yan, “Toward quantum simulation of non-markovian open quantum dynamics: A universal and compact theory,” *Physical Review A* **110**, 032620 (2024).
- ⁷L. Han, V. Chernyak, Y.-A. Yan, X. Zheng, and Y. Yan, “Stochastic representation of non-markovian fermionic quantum dissipation,” *Physical review letters* **123**, 050601 (2019).
- ⁸K. Song, L. Song, and Q. Shi, “An alternative realization of the exact non-markovian stochastic schrödinger equation,” *The Journal of Chemical Physics* **144** (2016).
- ⁹D. Segal, “Thermal conduction in molecular chains: Non-markovian effects,” *The Journal of chemical physics* **128** (2008).
- ¹⁰B. J. Berne and G. Harp, “On the calculation of time correlation functions,” *Advances in chemical physics* , 63–227 (1970).
- ¹¹A. Bednorz, W. Belzig, and A. Nitzan, “Nonclassical time correlation functions in continuous quantum measurement,” *New Journal of Physics* **14**, 013009 (2012).
- ¹²J. Cao and G. A. Voth, “Semiclassical approximations to quantum dynamical time correlation functions,” *The Journal of chemical physics* **104**, 273–285 (1996).
- ¹³Q. Shi and E. Geva, “A relationship between semiclassical and centroid correlation functions,” *The Journal of chemical physics* **118**, 8173–8184 (2003).
- ¹⁴Y. Wang, Z.-H. Chen, R.-X. Xu, X. Zheng, and Y. Yan, “A statistical quasi-particles thermofield theory with gaussian environments: System–bath entanglement theorem for nonequilibrium correlation functions,” *The Journal of Chemical Physics* **157** (2022).
- ¹⁵W. Liu, J. Chen, and W. Dou, “Polaritons under extensive disordered gas-phase molecular rotations in a fabry–pérot cavity,” *The Journal of Physical Chemistry C* **128**, 12544–12550 (2024).
- ¹⁶W. Liu, R.-H. Bi, C. Zhao, Y. Wang, and W. Dou, “Absorption spectra with kernel polynomial neural quantum states,” *The Journal of Physical Chemistry Letters* **16**, 12216–12222 (2025).
- ¹⁷A. Montoya-Castillo and D. R. Reichman, “Approximate but accurate quantum dynamics from the mori formalism. ii. equilibrium time correlation functions,” *The Journal of chemical physics* **146** (2017).
- ¹⁸M. Thoss, H. Wang, and W. H. Miller, “Generalized forward–backward initial value representation for the calculation of correlation functions in complex systems,” *The Journal of Chemical Physics* **114**, 9220–9235 (2001).
- ¹⁹Y. Yan, J. Jin, R.-X. Xu, and X. Zheng, “Dissipation equation of motion approach to open quantum systems,” *Frontiers of Physics* **11**, 110306 (2016).

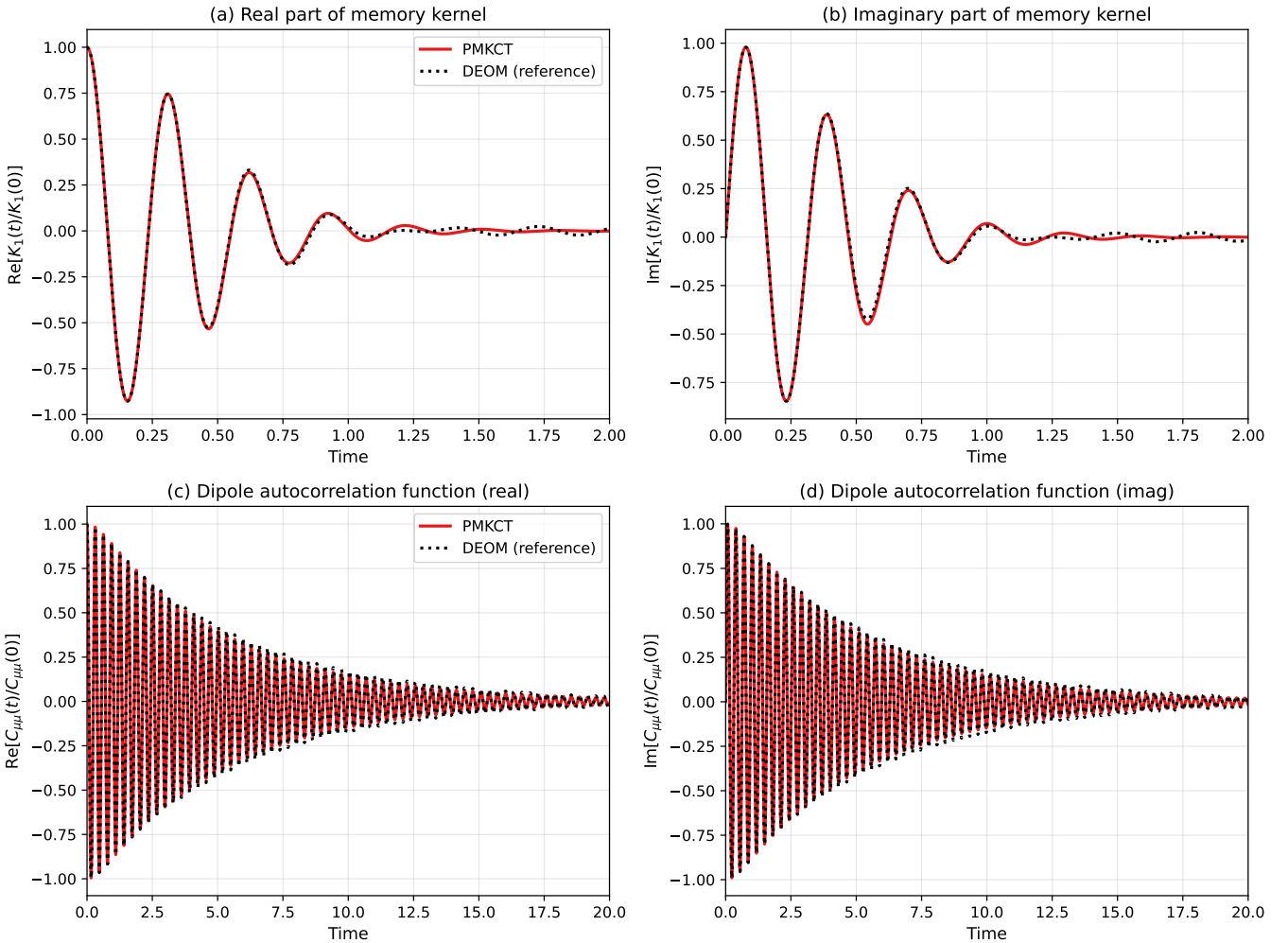


FIG. 2: Time evolution for the spin-boson model (parameters as in Fig. 1). Solid lines: PMKCT with $N = 40$. Dotted lines: Reference DEOM calculation.

²⁰N. Makri, “Numerical path integral techniques for long time dynamics of quantum dissipative systems,” *Journal of Mathematical Physics* **36**, 2430–2457 (1995).

²¹D. E. Makarov and N. Makri, “Path integrals for dissipative systems by tensor multiplication. condensed phase quantum dynamics for arbitrarily long time,” *Chemical physics letters* **221**, 482–491 (1994).

²²A. G. Redfield, “On the theory of relaxation processes,” *IBM Journal of Research and Development* **1**, 19–31 (1957).

²³M. Tokuyama and H. Mori, “Statistical-mechanical theory of the boltzmann equation and fluctuations in μ space,” *Progress of Theoretical Physics* **56**, 1073–1092 (1976).

²⁴G. Cohen and M. Galperin, “Green’s function methods for single molecule junctions,” *The Journal of chemical physics* **152** (2020).

²⁵J. C. Tully, “Molecular dynamics with electronic transitions,” *The Journal of Chemical Physics* **93**, 1061–1071 (1990).

²⁶C. F. Craig, W. R. Duncan, and O. V. Prezhdo, “Trajectory surface hopping in the time-dependent kohn-sham approach for electron-nuclear dynamics,” *Physical review letters* **95**, 163001 (2005).

²⁷L. Wang, A. Akimov, and O. V. Prezhdo, “Recent progress in surface hopping: 2011–2015,” *The journal of physical chemistry letters* **7**, 2100–2112 (2016).

²⁸J. R. Mannouch and J. O. Richardson, “A mapping approach to surface hopping,” *The Journal of Chemical Physics* **158** (2023).

²⁹Y. Wang, R. Bi, W. Liu, J. Han, and W. Dou, “Mixed quantum-classical approaches to spin current and polarization dynamics in chiral molecular junctions,” *The Journal of Physical Chemistry Letters* (2025).

³⁰S. Nakajima, “On quantum theory of transport phenomena: Steady diffusion,” *Progress of Theoretical Physics* **20**, 948–959 (1958).

³¹R. Zwanzig, “Ensemble method in the theory of irreversibility,” *The Journal of Chemical Physics* **33**, 1338–1341 (1960).

³²H. Mori, “Transport, collective motion, and brownian motion,” *Progress of theoretical physics* **33**, 423–455 (1965).

³³D. Brian and X. Sun, “Generalized quantum master equation: A tutorial review and recent advances,” *Chinese Journal of Chemical Physics* **34**, 497–524 (2021).

³⁴L. Kidon, H. Wang, M. Thoss, and E. Rabani, “On the memory kernel and the reduced system propagator,” *The Journal of chemical physics* **149** (2018).

³⁵W. Liu, Y. Su, Y. Wang, and W. Dou, “Memory kernel coupling theory: Obtaining time correlation function from higher-order moments,” *Physical Review Letters* **135**, 148001 (2025).

³⁶R.-H. Bi, W. Liu, and W. Dou, “Universal structure of computing moments for exact quantum dynamics: Application to arbit-

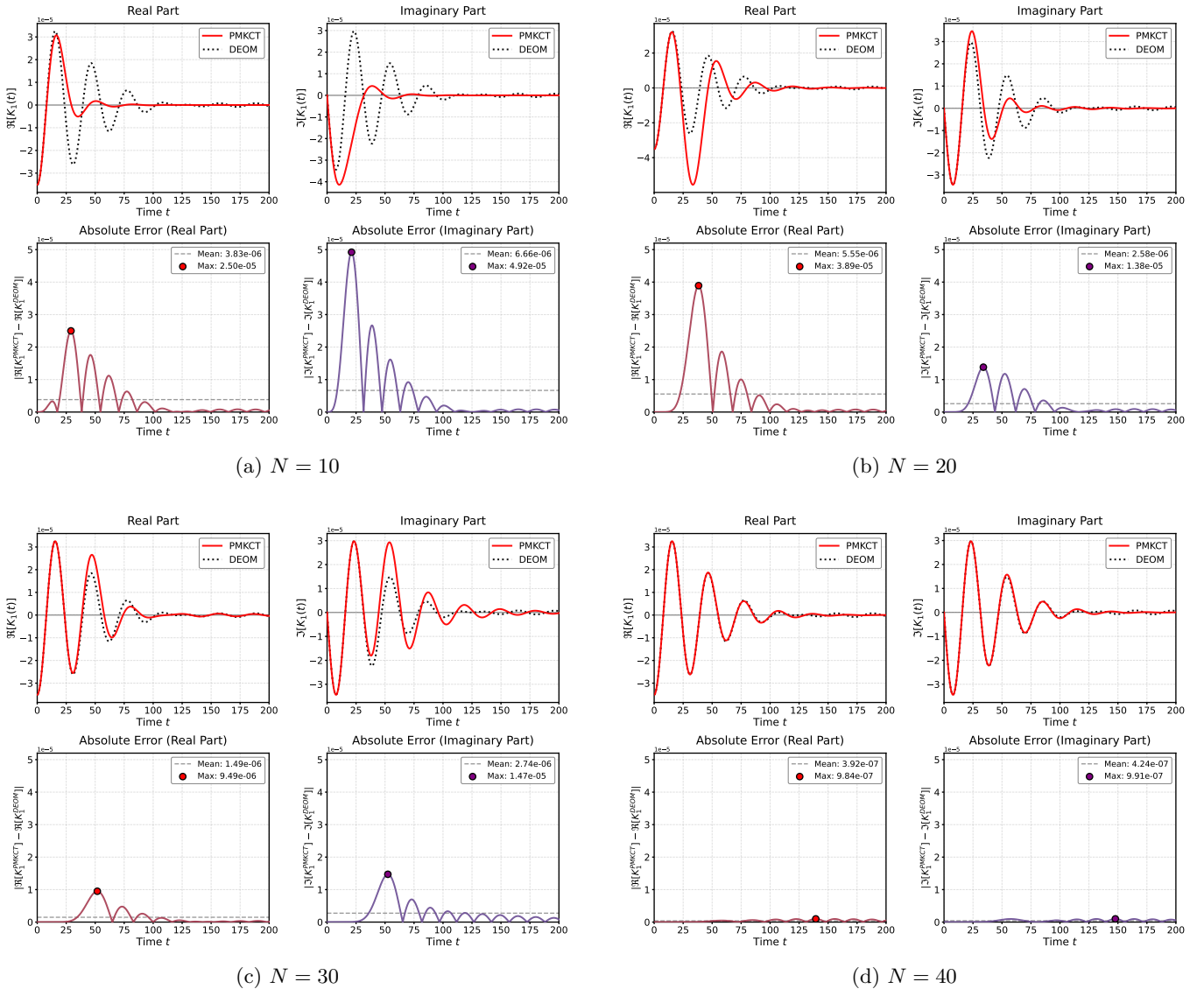


FIG. 3: Convergence of $K_1(t = 5)$ with truncation order N in PMKCT for different values: (a) $N = 10$, (b) $N = 20$, (c) $N = 30$, (d) $N = 40$.

trary system–bath couplings,” The Journal of Chemical Physics **162** (2025).

³⁷A. Akbari, M. J. Hashemi, A. Rubio, R. Nieminen, and R. van Leeuwen, “Challenges in truncating the hierarchy of time-dependent reduced density matrices equations,” Physical Review B—Condensed Matter and Materials Physics **85**, 235121 (2012).

³⁸Z. Tang, X. Ouyang, Z. Gong, H. Wang, and J. Wu, “Extended hierarchy equation of motion for the spin-boson model,” The Journal of Chemical Physics **143** (2015).

³⁹S. Bai, S. Zhang, C. Huang, and Q. Shi, “Hierarchical equations of motion for quantum chemical dynamics: Recent methodology developments and applications,” Accounts of Chemical Research **57**, 3151–3160 (2024).

⁴⁰W. Liu, Z.-H. Chen, Y. Su, Y. Wang, and W. Dou, “Predicting rate kernels via dynamic mode decomposition,” The Journal of

Chemical Physics **159** (2023).

⁴¹J. C. A. Barata and M. S. Hussein, “The moore–penrose pseudoinverse: A tutorial review of the theory,” Brazilian Journal of Physics **42**, 146–165 (2012).

⁴²R. MacAusland, “The moore–penrose inverse and least squares,” Math 420: Advanced Topics in Linear Algebra , 1–10 (2014).

⁴³L. N. Trefethen and D. Bau, *Numerical linear algebra* (SIAM, 2022).

⁴⁴G. H. Golub and C. F. Van Loan, *Matrix computations* (JHU press, 2013).

⁴⁵J. C. Butcher, *Numerical methods for ordinary differential equations* (John Wiley & Sons, 2016).

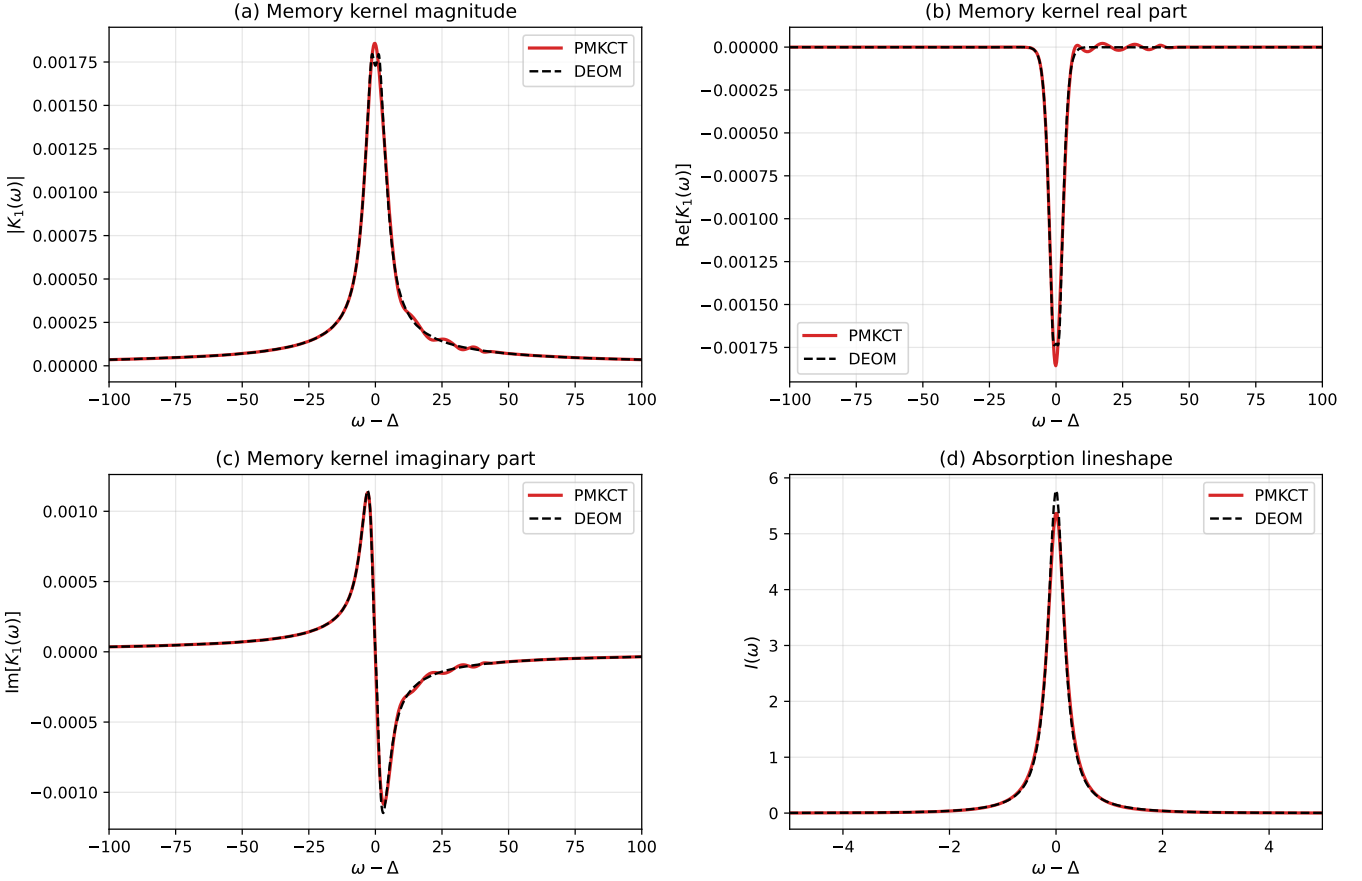


FIG. 4: Frequency-domain results. (a) Memory kernel magnitude. (b) Memory kernel real part. (c) Memory kernel imaginary part. (d) Absorption lineshape. Parameters as in previous figures.